Molecule Design and Isomorphism Synthesis Towards Artificial Enzyme

(Supporting information)

Experimental Section

Materials and general methods. All chemicals were commercially purchased and used as supplied. Elemental analyses of C, H, and N were performed using an EA1110 elemental analyzer. The IR spectrum was recorded in the range 4000-400 cm^{-1} on a HYPERION spectrometer with a pressed KBr pellet. The TG-DTA analysis was carried out by Universal Analysis 2000 thermogravimetric analyzer (TGA) in N_2 with a heating rate of 10 °C /min. The powder X-ray diffraction (PXRD) data was collected on an X'Pert-ProMPD (Holand) D/max-γA X-ray diffractometer with Cu Kα radiation in a flat plate geometry. Crystal data were collected on a Bruker X8 APEX II-CCD single crystal X-ray diffractometer with Mo Kα radiation (λ = 0.71073Å).

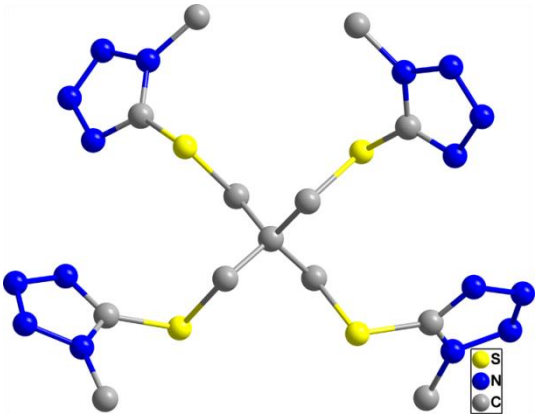

Scheme S1. The bpbb ligand used in this report.

Synthesis of $Cu_3(bpbb)_2(PW_{12}O_{40})\cdot 3H_2O$ (1): A mixture of $CuAc_2\cdot H_2O$ (0.12 g, 0.60mmol), bpbb (0.08 g, 0.15 mmol), $H_3PW_{12}O_{40}\cdot nH_2O$ (0.29 g, 0.10 mmol) was dissolved in 10 mL of distilled water at room temperature. When the pH value of the mixture was adjusted to about 1.9 with 1.0 $mol\cdot L^{-1}$ $HClO_4$, the suspension was put into a 15 ml Teflon-lined autoclave and kept under autogenous pressure at 160 °C for 3 days. After cooling to room temperature slowly, brown crystals of compound **1** were filtered and washed with distilled water (Yields 68% based on W). Anal. Calcd for $C_{26}H_{46}Cu_3N_{32}O_{43}S_8PW_{12}$: C 7.47, H 1.10, N 10.73, P 0.74, W 52.79, Cu 4.56 %. Found: C 7.52, H 1.15, N 10.68, P 0.66, W 52.70, Cu 4.61 %. IR (KBr pellet, cm^{-1}): 1609, 1410, 1275, 1180, 1078, 978, 893, 814. CCDC number 878793.

Synthesis of $[Cu_4(bpbb)_2(SiW_{12}O_{40})(H_2O)_2]\cdot H_2O$ (2): It was prepared in a manner similar to that for compound **1**, but the POMs $H_4SiW_{12}O_{40}\cdot nH_2O$ (0.29 g, 0.10 mmol) was used instead of $H_3PW_{12}O_{40}\cdot nH_2O$. When the pH value of the mixture was adjusted to about 2.4 with 1.0 $mol\cdot L^{-1}$ $HClO_4$, the suspension was put into a 15 ml Teflon-lined autoclave and kept under autogenous pressure at 160 °C for 3 days. After cooling to room temperature slowly, orange crystals of compound **2** were filtered and washed with distilled water (Yields 75% based on W). Anal. Calcd

for $C_{26}H_{46}Cu_4N_{32}O_{43}S_8SiW_{12}$: C 7.37, H 1.09, N 10.57, Si 0.66, W 52.04, Cu 5.99 %. Found: C 7.45, H 1.14, N 10.48, Si 0.61, W 52.15, Cu 5.87 %. IR (KBr pellet, cm^{-1}): 1620, 1439, 1277, 1182, 1013, 972, 920, 797. CCDC number 878794.

Synthesis of $Cu_3(bpbb)_2(PMo_{12}O_{40})\cdot 3H_2O$ (3): It was prepared in a manner similar to that for compound **1**, but the POMs $H_3PMoO_{40}\cdot nH_2O$ (0.18g, 0.10 mmol) was used instead of $H_3PW_{12}O_{40}\cdot nH_2O$. When the pH value of the mixture was adjusted to about 2.4 with 1.0 $mol\cdot L^{-1}$ $HClO_4$, the suspension was put into a 15 ml Teflon-lined autoclave and kept under autogenous pressure at 160 °C for 3 days. After cooling to room temperature slowly, black crystals of compound **3** were filtered and washed with distilled water (Yields 85% based on Mo). Anal. Calcd for $C_{26}H_{46}Cu_3N_{32}O_{43}S_8PMo_{12}$: C 9.99, H 1.47, N 14.35, P 0.99, Mo 36.86, Cu 6.10 %. Found: C 10.05, H 1.53, N 14.28, P 0.94, Mo 36.94, Cu 6.02 %. IR (KBr pellet, cm^{-1}): 1618, 1404, 1277, 1180, 1059, 957, 874, 804. CCDC number 878795.

Synthesis of $[Cu_4(bpbb)_2(SiMo_{12}O_{40})(H_2O)_2]\cdot H_2O$ (4): It was prepared in a manner similar to that for compound **1**, but the POMs $H_4SiMo_{12}O_{40}\cdot nH_2O$ (0.18 g, 0.10 mmol) was used instead of $H_3PW_{12}O_{40}\cdot nH_2O$. When the pH value of the mixture was adjusted to about 2.4 with 1.0 $mol\cdot L^{-1}$ $HClO_4$, the suspension was put into a 15 ml Teflon-lined autoclave and kept under autogenous pressure at 160 °C for 3 days. After cooling to room temperature slowly, black crystals of compound **4** were filtered and washed with distilled water (Yields 80% based on Mo). Anal. Calcd for $C_{26}H_{46}Cu_4N_{32}O_{43}S_8SiMo_{12}$: C 9.81, H 1.44, N 14.07, Si 0.97, Mo 36.16, Cu 7.98 %. Found: C 9.87, H 1.35, N 14.15, Si 0.89, Mo 36.10, Cu 8.09 %. IR (KBr pellet, cm^{-1}): 1618, 1404, 1277, 1180, 947, 901, 795. CCDC number 878796.

Crystal Structure of Compound 1. Single crystal X-ray analysis shows that the structure of compound **1** contains one $[PW_{12}O_{40}]^{3-}$ (abbreviated as PW_{12}) polyoxoanion, two types of bpbb ligands ($bpbb^1$, $bpbb^2$), three kinds of Cu^+ ions (Cu1, Cu2, Cu3) and three lattice water molecules in the crystallographically independent unit (Fig. S1). Analysis of the bond valence sum calculations (BVS) suggests that all the copper ions are in the +I oxidation state.

In compound **1**, the PW_{12} polyanion is two coordinated by Cu1 and Cu3 atoms through the terminal O13 and bridging O21 atoms (Fig. S2). There are two crystallographically independent bpbb ligands ($bpbb^1$, $bpbb^2$) in compound **1**, which exhibit two kinds of coordination geometries (Fig. S3). Each $bpbb^1$ ligand provides six N-donors to coordinate four copper ions (one Cu1, one Cu2 and two Cu3 ions). While the $bpbb^2$ ligand acts as a linker to coordinate three copper ions (one Cu1 and two Cu2 ions). It is worthy noting that a tetrazolate ring is not coordinated in the $bpbb^2$ ligand. In addition, three kinds of Cu^+ ions with different coordination patterns are existed in compound **1** (Fig. S4). Due to the strong Jahn–Teller effect of the d^9 electronic configuration, the Cu1 ion adopts a tetrahedron geometry which is completed by three nitrogen atoms (N1, N5 from bpbb1 ligand and N18 from $bpbb^2$ ligand), and one terminal oxygen atom (O13) from PW_{12} polyoxoanions. Cu2 ion exhibits a similar coordination environment to Cu1 ion except that the three nitrogen atoms (N9, N13, N14) are from two $bpbb^2$ ligands and one bridging oxygen atom (O21) from the PW_{12} polyoxoanions. While Cu3 ion is coordinated by one nitrogen atom (N6) from the $bpbb^1$ ligand and three nitrogen atom (N17, N25, N30) from two $bpbb^2$ ligands (Fig. S3). The bond distances around the Cu^+ ions are normal.

Further crystal structure analysis reveals that compound **1** is constructed by two dimeric structures (dimer-1 and dimer-2). Dimer-1 is formed by two $bpbb^1$ ligands and two PW_{12} anions arraying in a circle by sharing four Cu^+ ions (two Cu1 and two Cu3 ions) (Fig. S5). Furthermore,

the dimer-1 structures connect to each other via sharing two Cu3 ions to generate a straight chain (Fig. S6). These straight chains pack in parallel in the ac plane. The dimer-2 is formed by two $bpbb^{2}$ ligands which connect with each other by sharing two Cu2 ions. These dimer-2 units span the channels between neighboring chains and keep them link together by sharing four Cu^{+} ions (two Cu1 and two Cu2 ions) with them, yielding a 2D layer (Fig. S7).

Crystal Structure of Compound 2. Crystal structure analysis reveals that compound **2** also exhibits a 2D layer, which is constructed by one $[SiW_{12}O_{40}]^{4-}$ (abbreviated as SiW_{12}) polyoxoanion, two types of bpbb ligands with different coordination patterns ($bpbb^{3}$, $bpbb^{4}$), four kinds of Cu cations (Cu1, Cu2, Cu3, Cu4) and one lattice water molecules in the asymmetric unit (Fig. S8-9).

The basic structure of compound **2** is similar to compound **1** expect one Cu^{+} ion different. This additional Cu^{+} (Cu4) ion adopts a four-coordinated trigonal-pyramidal geometry of $[Cu_{(4)}N_2O_2]$ by two N atoms from two bpbb ligands (N2 atom from $bpbb^{3}$ ligand; N22 atom from $bpbb^{4}$ ligand) and two O atoms from two lattice water molecules (Fig. S11). As a result, the $bpbb^{1}$ ligand in compound **1** is replaced by $bpbb^{3}$ ligand in compound **2**, and $bpbb^{2}$ ligand is replaced by $bpbb^{4}$ ligand (Fig. S12). Each $bpbb^{3}$ ligand provides seven N-donors to coordinate five copper ions (one Cu1, one Cu2, one Cu4 and two Cu3 ions). And the $bpbb^{4}$ ligand is connected four copper ions (one Cu1, one Cu4 and two Cu2 ions) in a bridging mode.

In other words, the compound **2** is constructed by another two dimeric structures (dimer-3 and dimer-4). Dimer-3 is formed by two $bpbb^{3}$ ligands and two SiW_{12} anions arraying in a circle by sharing four Cu atoms (two Cu1 and two Cu3 ions) (Fig. S13). The dimer-4 is formed by two $bpbb^{4}$ ligands connected together by sharing two Cu2 ions. Furthermore, the relationship between dimer-3 structures and dimer-4 units is similar to it between dimer-1 structures and dimer-2 units (Fig. S14-15).

Crystal Structure of Compound 3. Crystal analysis shows that the structure of compound **3** contains one $[PMo_{12}O_{40}]^{3-}$ (abbreviated as PMo_{12}) polyoxoanion, two types of bpbb ligands with different coordination patterns ($bpbb^{5}$, $bpbb^{6}$), three kinds of Cu cations (Cu1, Cu2, Cu3) and three lattice water molecules in the crystallographically independent unit (Fig. S16). In other words, compound **3** has the same structure as compound **1** except that the PW_{12} anion is replaced by the PMo_{12} anion. As a result, the dimer-1 is replaced by dimer-5 and dimer-2 is replaced by dimer-6 (Fig. S17-22).

Crystal Structure of Compound 4. Crystal structure analysis reveals that compound **4** is constructed by one $[SiMo_{12}O_{40}]^{4-}$ (abbreviated as $SiMo_{12}$) polyoxoanion, two types of bpbb ligands with different coordination patterns ($bpbb^{7}$, $bpbb^{8}$), four kinds of Cu cations (Cu1, Cu2, Cu3, Cu4) and one lattice water molecules in the asymmetric unit (Fig. S23). In other words, compound **4** has the same structure as compound **2** except that the SiW_{12} anion is replaced by the $SiMo_{12}$ anion. As a result, the dimer-3 is replaced by dimer-7 and dimer-4 is replaced by dimer-8 (Fig. S24-29).

Table S1. Crystal Data and Structural Refinements for compounds **1**-**4**.

	1	**2**	**3**	**4**
formula	$C_{26}H_{46}Cu_3N_{32}O_{43}S_8PW_{12}$	$C_{26}H_{46}Cu_4N_{32}O_{43}S_8SiW_{12}$	$C_{26}H_{46}Cu_3N_{32}O_{43}S_8PMo_{12}$	$C_{26}H_{46}Cu_4N_{32}O_{43}S_8SiMo_{12}$
*F*w	4179.22	4239.88	3124.30	3184.96
crystal system	triclinic	triclinic	triclinic	triclinic
space group	*P*$\bar{1}$	*P*$\bar{1}$	*P*$\bar{1}$	*P*$\bar{1}$
a (Å)	13.1028(11)	13.095(3)	13.063(3)	13.0057(7)
b (Å)	13.5056(11)	13.375(3)	13.512(4)	13.3497(8)
c (Å)	23.797(2)	23.823(5)	23.709(6)	23.6446(13)
α (deg)	92.405(2)	92.183(4)	92.366(6)	91.917(1)
β (deg)	91.395(1)	90.456(3)	91.564(5)	91.017(1)
γ (deg)	105.902(1)	105.986(3)	105.990(5)	106.702(1)
V (Å^3)	4043.6(6)	4007.8(14)	4016.3(18)	3928.2(4)
Z	2	2	2	2
*D*c (g/cm^3)	3.432	3.513	2.584	2.693
μ (mm^{-1})	18.091	18.506	2.916	3.240
F(000)	3776.0	3832.0	3008.0	3064.0
collcd reflns	53668	54724	55203	52951
unique reflns	14130	14018	13998	13747
obsd reflns	12869	11948	12119	12994
no. of param	1134	1145	1134	1152
R_{int}	0.041	0.035	0.024	0.017
Temperature (K)	296	296	296	150
GOF	1.034	1.048	1.045	1.034
R_1[a] [I > 2σ(I)]	0.0267	0.0287	0.0242	0.0554
wR_2[b] (all data)	0.0686	0.0766	0.0637	0.1271

[a]$R_1 = \sum||F_o|-|F_c||/\sum|F_o|$; [b]$wR_2 = \sum[w(F_o^2-F_c^2)^2]/\sum[w(F_o^2)^2]^{1/2}$.

Table S2. Selected bond distances (Å) and angles (°) for compounds **1**-**4**.

Compound **1**			
Cu(1)-N(5)	1.97(3)	Cu(2)-N(25)	2.04(4)
Cu(1)-N(1)	1.97(4)	Cu(2)-N(30)#1	2.06(3)
Cu(1)-N(18)	2.08(3)	Cu(3)-N(13)	1.93(3)
Cu(1)-O(13)	2.33(3)	Cu(3)-N(9)	1.96(3)
Cu(2)-N(17)	2.00(3)	Cu(3)-N(14)#2	2.15(3)
Cu(2)-N(6)	2.04(3)		
N(5)-Cu(1)-N(1)	137.8(14)	N(6)-Cu(2)-N(25)	101.1(13)
N(5)-Cu(1)-N(18)	108.7(13)	N(17)-Cu(2)-N(30)#1	110.1(14)
N(1)-Cu(1)-N(18)	110.6(14)	N(6)-Cu(2)-N(30)#1	108.8(14)
N(5)-Cu(1)-O(13)	97.6(11)	N(25)-Cu(2)-N(30)#1	94.3(14)
N(1)-Cu(1)-O(13)	97.7(12)	N(13)-Cu(3)-N(9)	146.5(14)
N(18)-Cu(1)-O(13)	89.3(12)	N(13)-Cu(3)-N(14)#2	108.6(13)
N(17)-Cu(2)-N(6)	107.2(14)	N(9)-Cu(3)-N(14)#2	100.0(13)

N(17)-Cu(2)-N(25)	133.4(14)		
Compound **2**			
Cu(1)-N(5)	1.978(8)	Cu(3)-N(9)	1.968(8)
Cu(1)-N(1)	2.006(8)	Cu(3)-N(14)#2	2.123(8)
Cu(1)-N(18)	2.062(8)	Cu(3)-O(21)#3	2.435(6)
Cu(1)-O(13)	2.247(6)	Cu(3')-N(9)	1.998(11)
Cu(2)-N(17)	2.000(8)	Cu(3')-N(13)	2.006(11)
Cu(2)-N(6)	2.047(8)	Cu(3')-N(14)#2	2.153(11)
Cu(2)-N(25)	2.050(8)	Cu(3')-S(3')	2.254(16)
Cu(2)-N(30)#1	2.074(8)	Cu(4)-N(22)	1.923(12)
Cu(3)-N(13)	1.967(8)	Cu(4)-N(2)	1.948(10)
N(5)-Cu(1)-N(1)	131.8(3)	N(13)-Cu(3)-N(14)#2	106.6(3)
N(5)-Cu(1)-N(18)	109.8(3)	N(9)-Cu(3)-N(14)#2	98.2(3)
N(1)-Cu(1)-N(18)	112.9(3)	N(13)-Cu(3)-O(21)#3	102.2(3)
N(5)-Cu(1)-O(13)	102.5(3)	N(9)-Cu(3)-O(21)#3	93.5(3)
N(1)-Cu(1)-O(13)	97.3(3)	N(14)#2-Cu(3)-O(21)#3	100.5(3)
N(18)-Cu(1)-O(13)	92.0(3)	N(9)-Cu(3')-N(13)	141.2(5)
N(17)-Cu(2)-N(6)	107.0(3)	N(9)-Cu(3')-N(14)#2	96.3(4)
N(17)-Cu(2)-N(25)	133.0(3)	N(13)-Cu(3')-N(14)#2	104.1(4)
N(6)-Cu(2)-N(25)	102.7(3)	N(9)-Cu(3')-S(3')	51.1(5)
N(17)-Cu(2)-N(30)#1	109.7(3)	N(13)-Cu(3')-S(3')	127.6(5)
N(6)-Cu(2)-N(30)#1	108.1(3)	N(14)#2-Cu(3')-S(3')	127.2(5)
N(25)-Cu(2)-N(30)#1	94.1(3)	N(22)-Cu(4)-N(2)	160.4(5)
N(13)-Cu(3)-N(9)	147.4(3)		
Compound **3**			
Cu(1)-N(1)	1.97(3)	Cu(2)-N(25)	2.04(3)
Cu(1)-N(5)	1.97(3)	Cu(2)-N(30)#1	2.07(3)
Cu(1)-N(18)	2.08(3)	Cu(3)-N(13)	1.94(3)
Cu(1)-O(13)	2.32(3)	Cu(3)-N(9)	1.96(3)
Cu(2)-N(17)	2.01(3)	Cu(3)-N(14)#2	2.17(3)
Cu(2)-N(6)	2.02(3)		
N(1)-Cu(1)-N(5)	137.5(13)	N(6)-Cu(2)-N(25)	101.1(13)
N(1)-Cu(1)-N(18)	110.6(13)	N(17)-Cu(2)-N(30)#1	109.6(13)
N(5)-Cu(1)-N(18)	108.6(12)	N(6)-Cu(2)-N(30)#1	108.9(13)
N(1)-Cu(1)-O(13)	99.0(11)	N(25)-Cu(2)-N(30)#1	94.6(13)
N(5)-Cu(1)-O(13)	97.3(11)	N(13)-Cu(3)-N(9)	144.9(12)
N(18)-Cu(1)-O(13)	89.1(11)	N(13)-Cu(3)-N(14)#2	107.7(11)
N(17)-Cu(2)-N(6)	107.3(13)	N(9)-Cu(3)-N(14)#2	99.3(12)
N(17)-Cu(2)-N(25)	133.5(13)		
Compound **4**			
Cu(1)-N(5)	1.973(7)	Cu(3)-O(21)#3	2.285(5)
Cu(1)-N(1)	1.986(7)	Cu(3')-N(13)	1.960(16)
Cu(1)-N(18)	2.048(7)	Cu(3')-N(9)	1.973(18)
Cu(1)-O(13)	2.229(6)	Cu(3')-N(14)#2	2.157(16)

Cu(2)-N(17)	1.990(7)	Cu(4)-N(22)	1.920(9)
Cu(2)-N(25)	2.027(7)	Cu(4)-N(2)	1.954(8)
Cu(2)-N(6)	2.028(7)	Cu(4)-O(2W)	2.214(7)
Cu(2)-N(30)#1	2.064(7)	Cu(4)-O(1W)	2.644(9)
Cu(3)-N(13)	1.950(7)	N(14)-Cu(3)#2	2.149(7)
Cu(3)-N(9)	1.985(7)	N(14)-Cu(3')#2	2.157(16)
Cu(3)-N(14)#2	2.149(7)	N(30)-Cu(2)#1	2.064(7)
N(5)-Cu(1)-N(1)	131.2(3)	N(9)-Cu(3)-N(14)#2	97.1(3)
N(5)-Cu(1)-N(18)	108.7(3)	N(13)-Cu(3)-O(21)#3	106.4(2)
N(1)-Cu(1)-N(18)	114.2(3)	N(9)-Cu(3)-O(21)#3	95.3(2)
N(5)-Cu(1)-O(13)	100.1(2)	N(14)#2-Cu(3)-O(21)#3	100.4(2)
N(1)-Cu(1)-O(13)	99.7(3)	N(13)-Cu(3')-N(9)	144.5(10)
N(18)-Cu(1)-O(13)	93.2(2)	N(13)-Cu(3')-N(14)#2	105.4(7)
N(17)-Cu(2)-N(25)	134.2(3)	N(9)-Cu(3')-N(14)#2	97.2(8)
N(17)-Cu(2)-N(6)	107.4(3)	N(22)-Cu(4)-N(2)	158.6(4)
N(25)-Cu(2)-N(6)	102.5(3)	N(22)-Cu(4)-O(2W)	90.0(3)
N(17)-Cu(2)-N(30)#1	108.9(3)	N(2)-Cu(4)-O(2W)	104.3(3)
N(25)-Cu(2)-N(30)#1	93.5(3)	N(22)-Cu(4)-O(1W)	96.8(3)
N(6)-Cu(2)-N(30)#1	107.9(3)	N(2)-Cu(4)-O(1W)	92.0(3)
N(13)-Cu(3)-N(9)	144.3(3)	O(2W)-Cu(4)-O(1W)	113.5(3)
N(13)-Cu(3)-N(14)#2	106.1(3)		

Symmetry code: for **1**: #1 -x+1, -y+1, -z+1; #2 -x+2, -y, -z; for **2**: #1 -x+1, -y+1, -z+1; #2 -x+2, -y, -z; #3 -x+1, -y, -z; for **3**: #1 -x+1, -y+1, -z+2; #2 -x+2, -y, -z+1; for **4**: #1 -x+2, -y+1, -z+1; #2 -x+1, -y+2, -z+2; #3 -x+2, -y+2, -z+2.

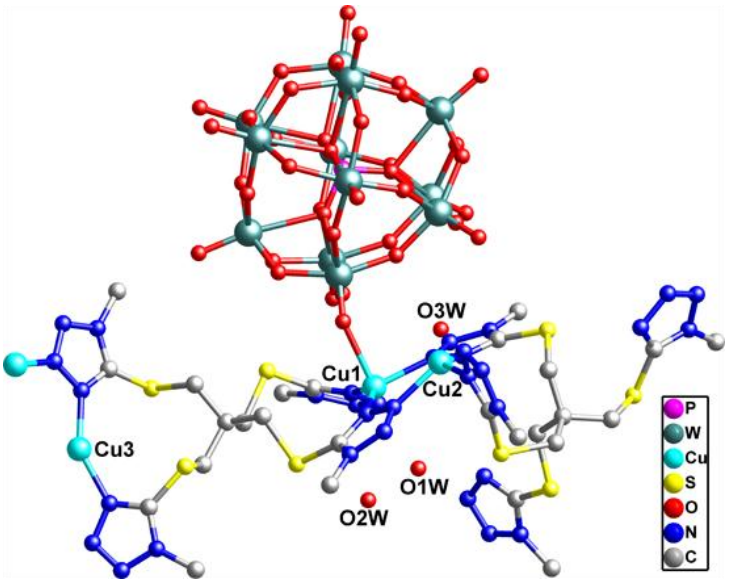

Fig. S1. Ball-and-stick view of the asymmetric unit of compound **1**. All H atoms are omitted for clarity.

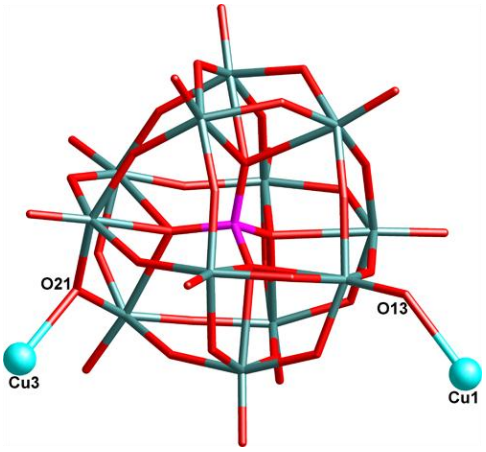

Fig. S2. View of coordination details of Keggin type polyoxoanion PW_{12} in compound **1**. Cu1 and Cu3 are coordinated atoms through the terminal O13 and bridging O21 atoms.

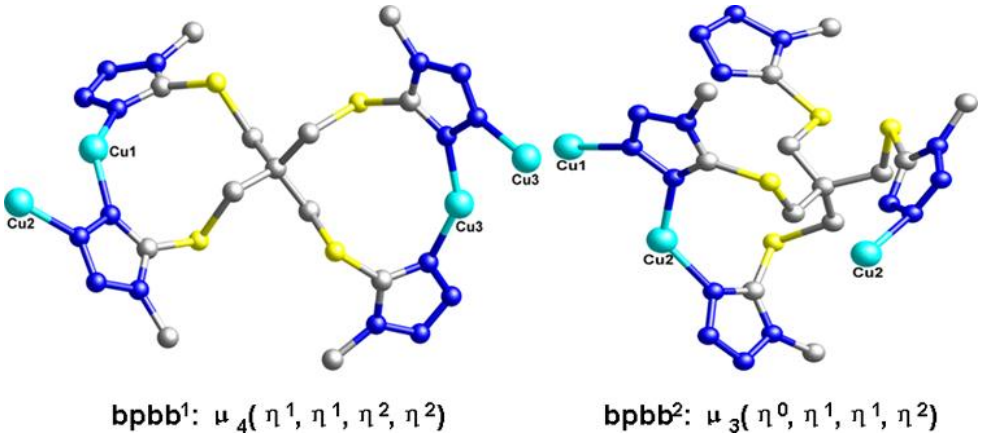

Fig. S3. The coordination modes of multiplex bpbb ligand in compound **1**.

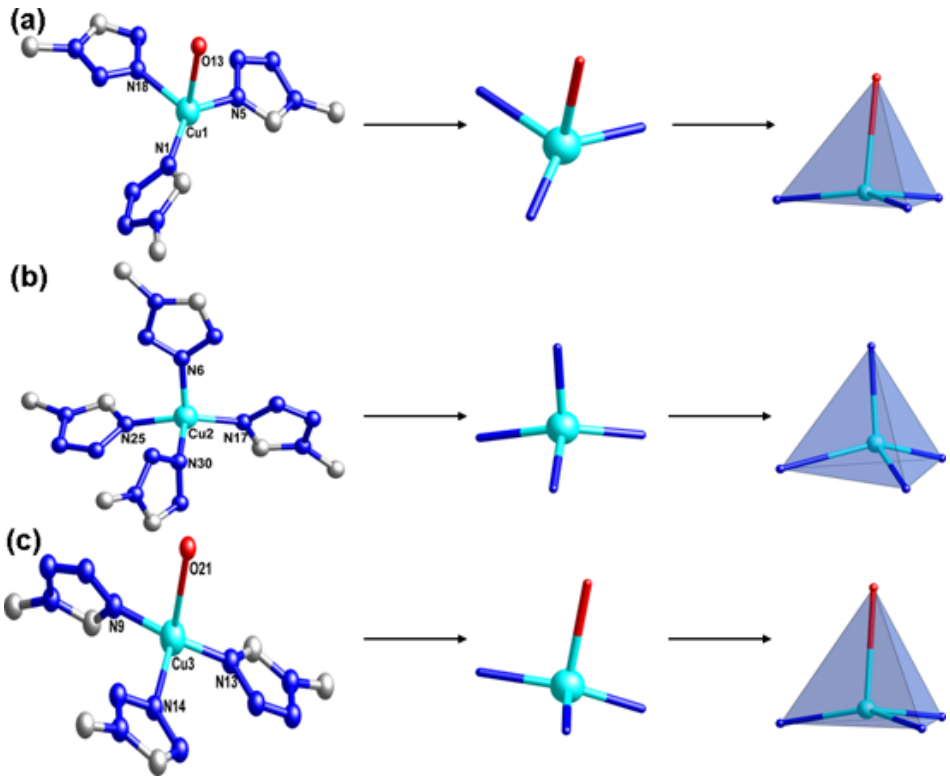

Fig. S4. The coordination details and modes of Cu^{+} ions in compound **1** (a) Cu1 (b) Cu2 (c) Cu3.

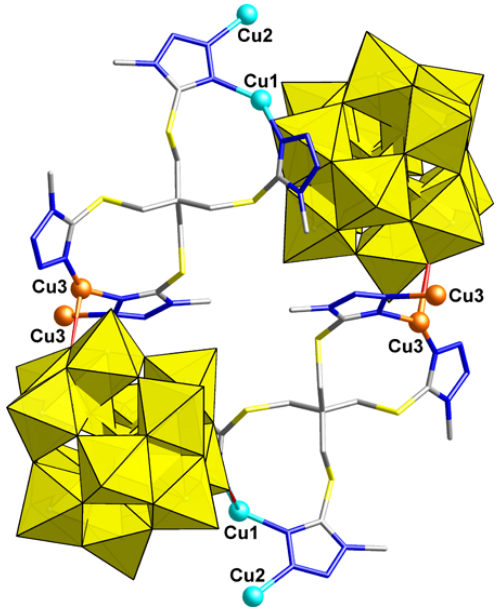

Fig. S5. Ball-and-stick and polyhedral representation of the dimer-1 structure in compound **1**.

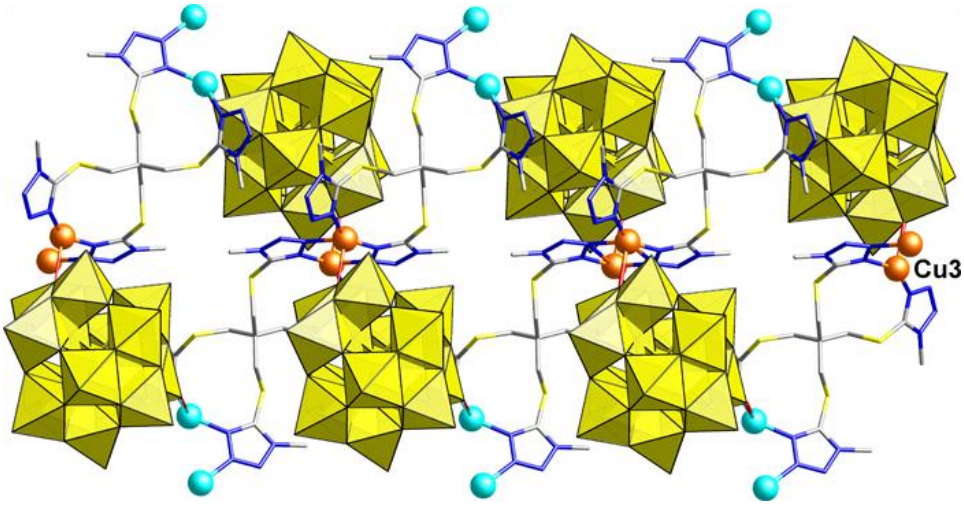

Fig. S6. The neighboring dimer-1 structures link together by sharing two Cu3 ions (orange) to form a straight chain in compound **1**.

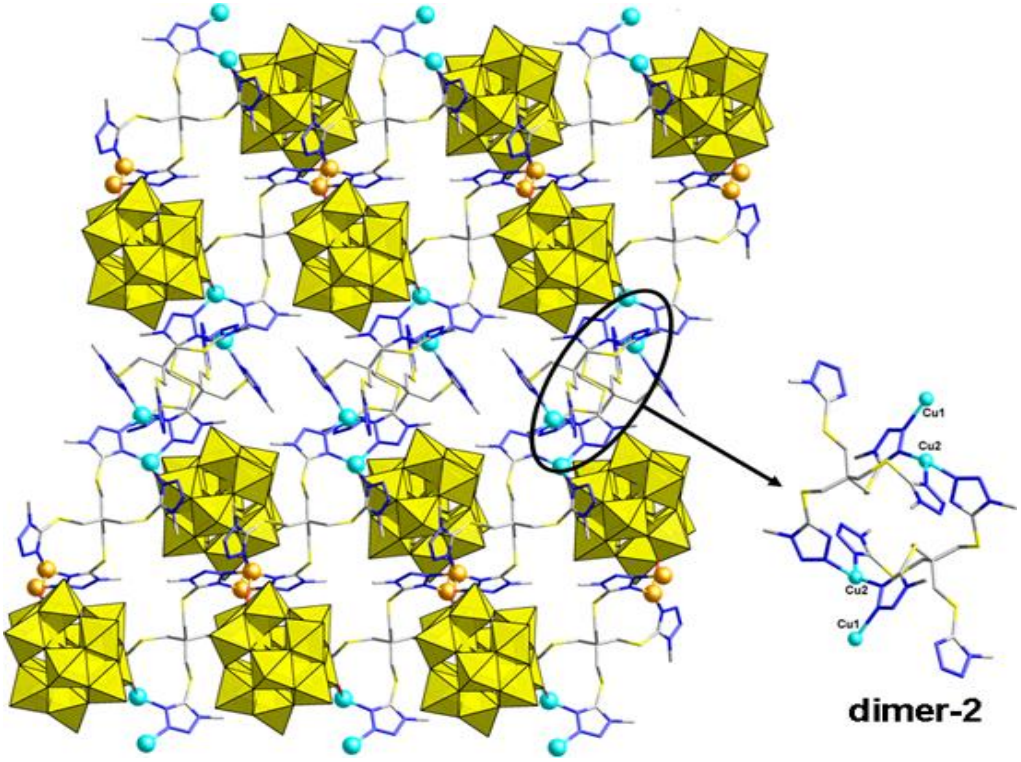

Fig. S7. Diagram illustrating the 2D layer in compound **1** which is constructed by straight chains and dimer-2 units. The dimer-2 unit is constructed by two bpbb[2] ligands.

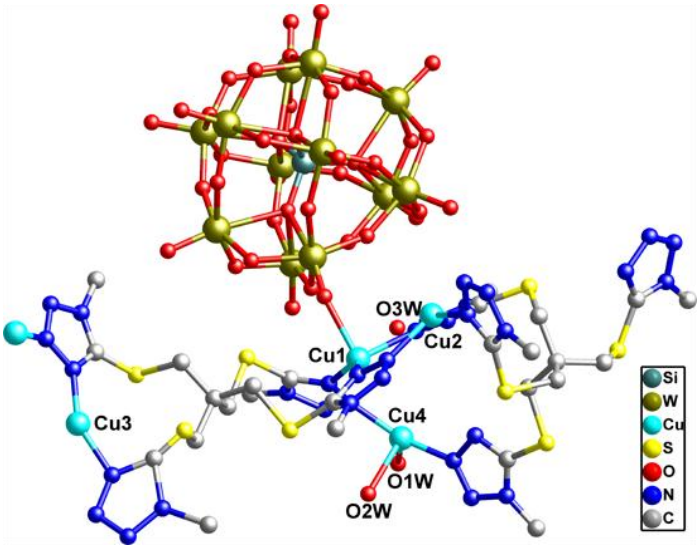

Fig. S8. Ball-and-stick view of the asymmetric unit of compound **2**. All H atoms are omitted for clarity.

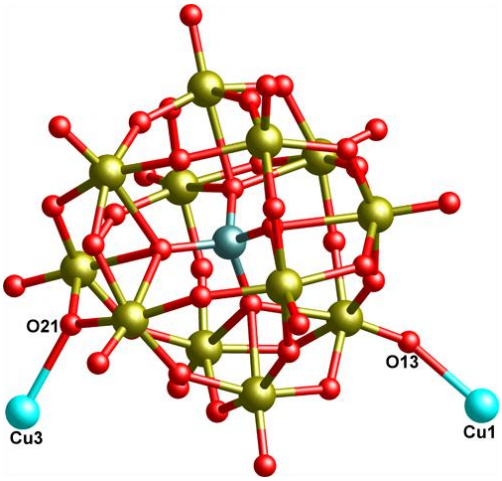

Fig. S9. View of coordination details of Keggin-type polyoxoanion SiW_{12} in compound **2**. Cu1 and Cu3 atoms are coordinated through the terminal O13 and bridging O21 atoms.

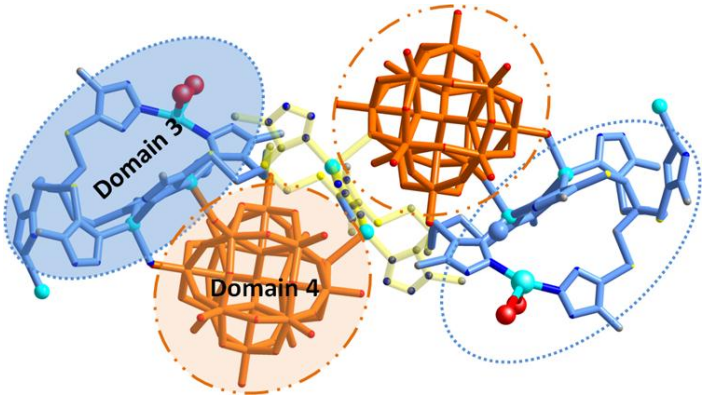

Fig. S10. Two structural domains (domain 3 and domain 4) included in compound **2**.

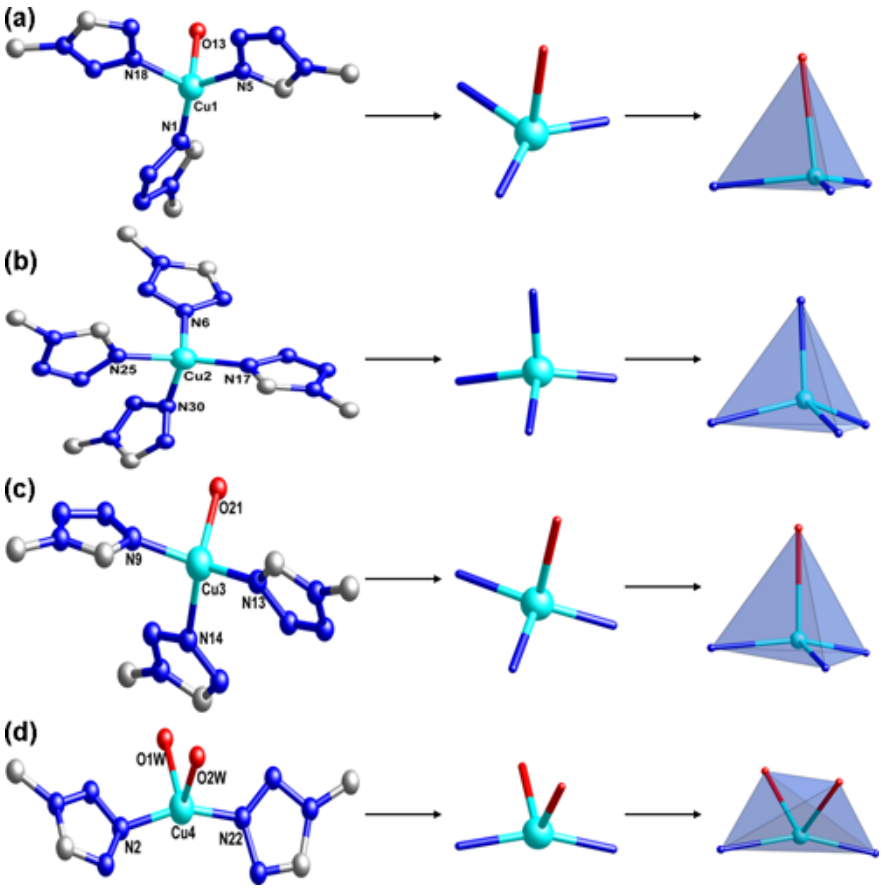

Fig. S11. The coordination details and modes of Cu^{+} ions in compound **2** (a) Cu1 (b) Cu2 (c) Cu3 (d) Cu4.

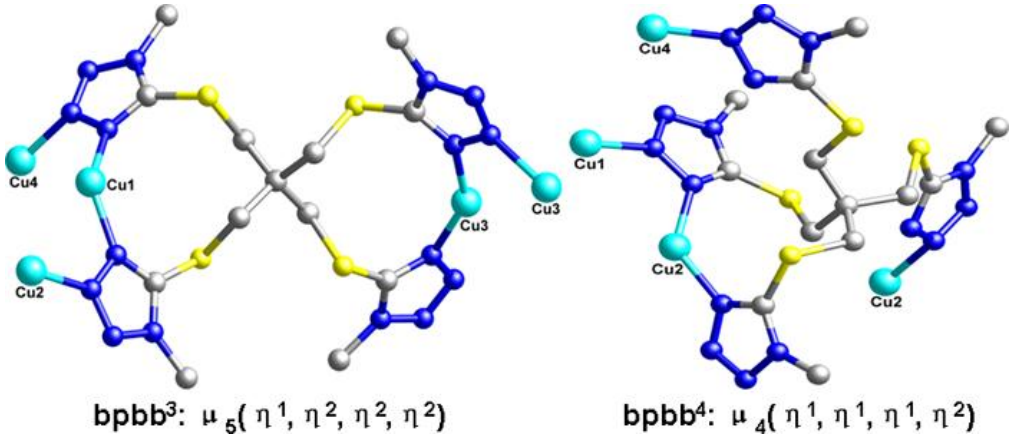

Fig. S12. The coordination modes of multiplex bpbb ligand in compound **2**.

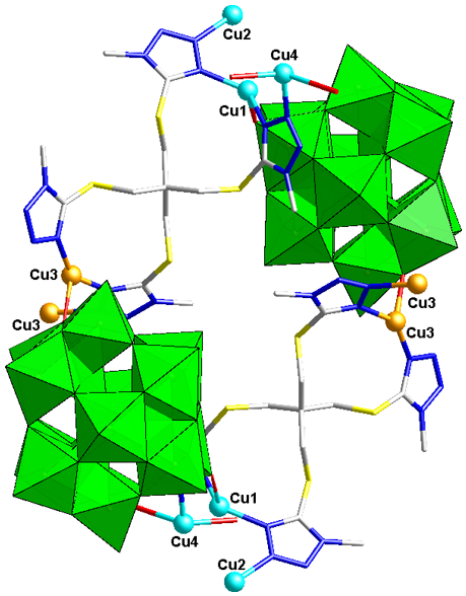

Fig. S13. Ball-and-stick and polyhedral representation of the dimer-3 structure in compound **2**.

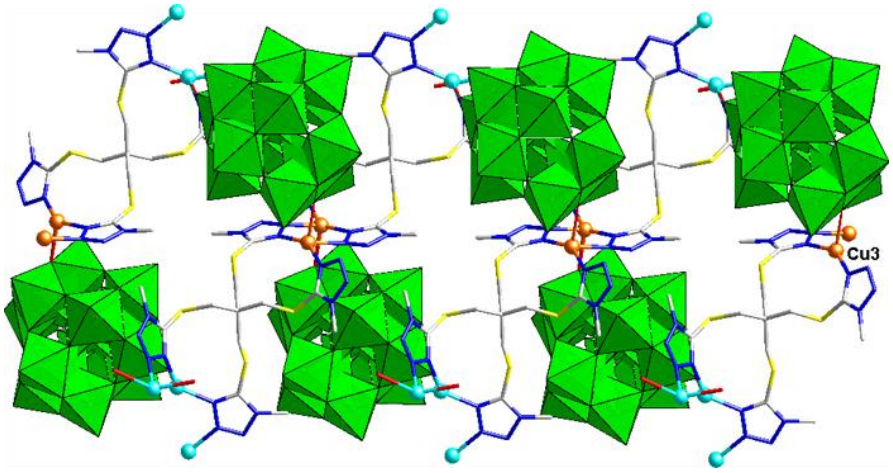

Fig. S14. The neighboring dimer-3 structures link together by sharing two Cu3 ions (orange) to generate a straight chain in compound **2**.

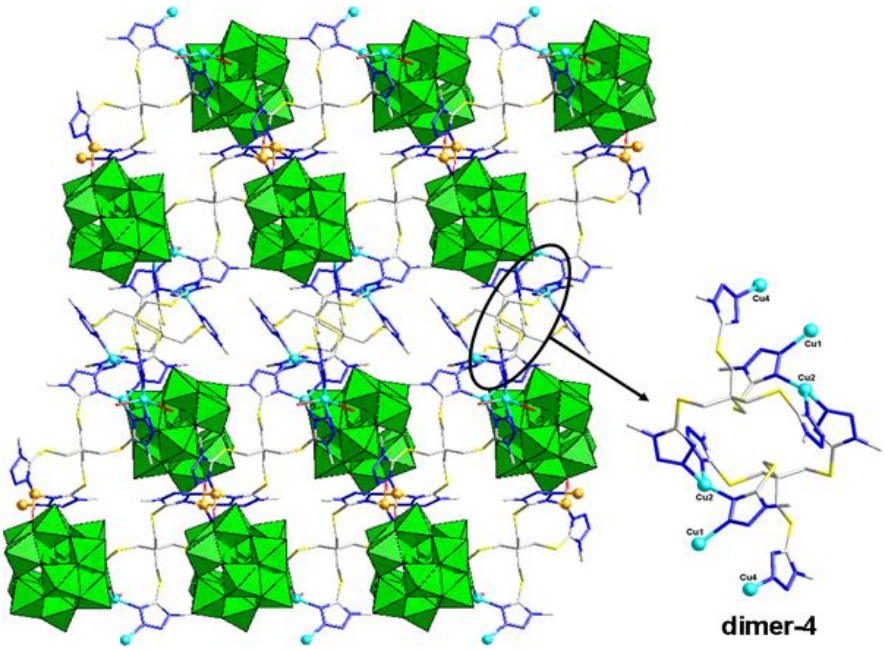

Fig. S15. Diagram illustrating the 2D layer in compound **2**, which is constructed by straight chains and dimer-4 units. The dimer-4 unit is constructed by two bpbb[4] ligands.

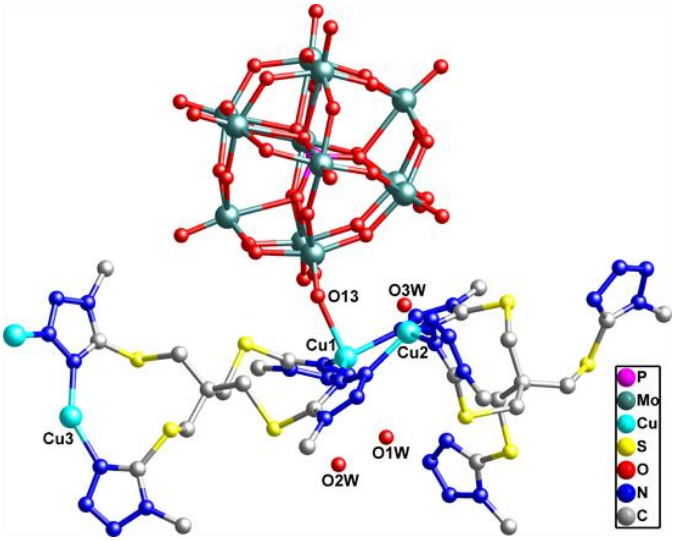

Fig. S16. Ball-and-stick view of the asymmetric unit of compound **3**. All H atoms are omitted for clarity.

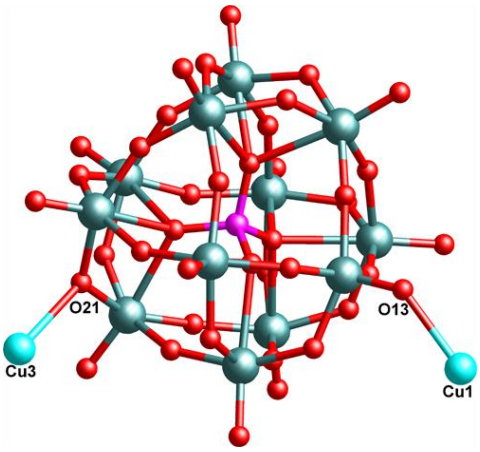

Fig. S17. View of coordination details of Keggin type polyoxoanion PMo_{12} in compound **3**. Cu1 and Cu3 atoms are coordinated through the terminal O13 and bridging O21 atoms.

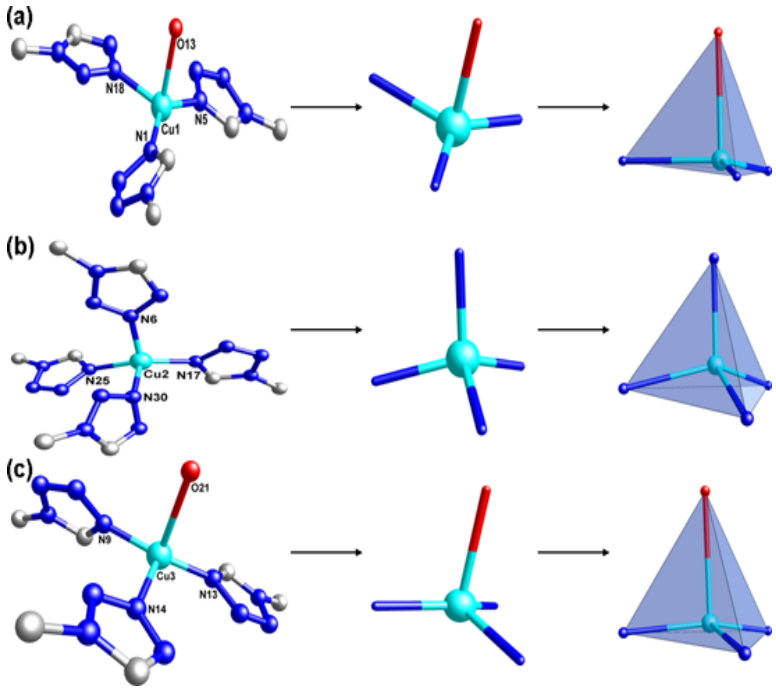

Fig. S18. The coordination details and modes of Cu^{+} ions in compound **3** (a) Cu1 (b) Cu2 (c) Cu3.

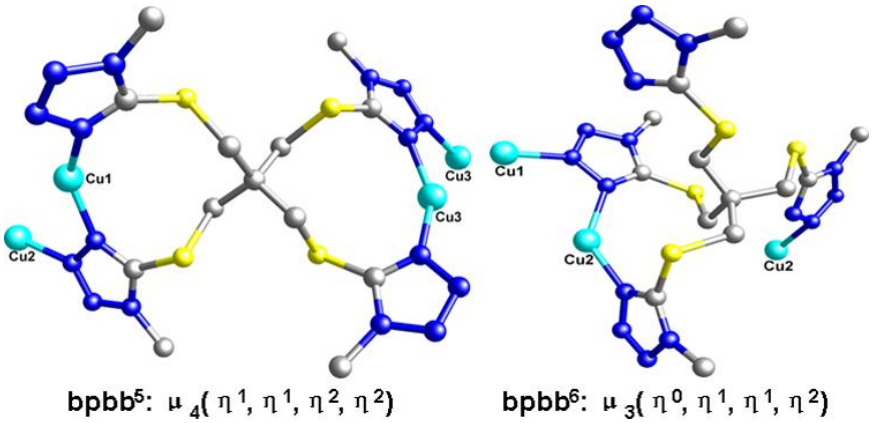

Fig. S19. The coordination modes of multiplex bpbb ligand in compound **3**.

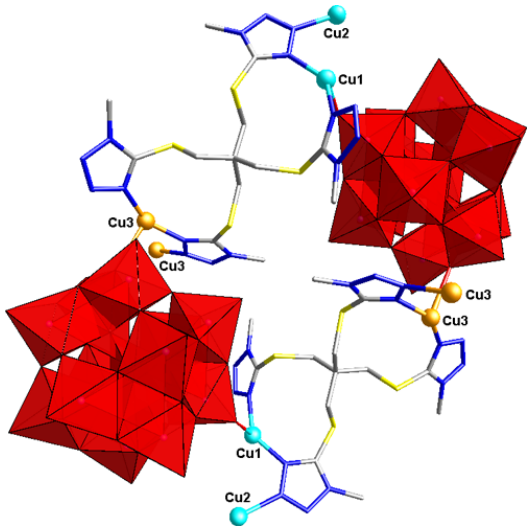

Fig. S20. Ball-and-stick and polyhedral representation of the dimer-5 structure in compound **3**.

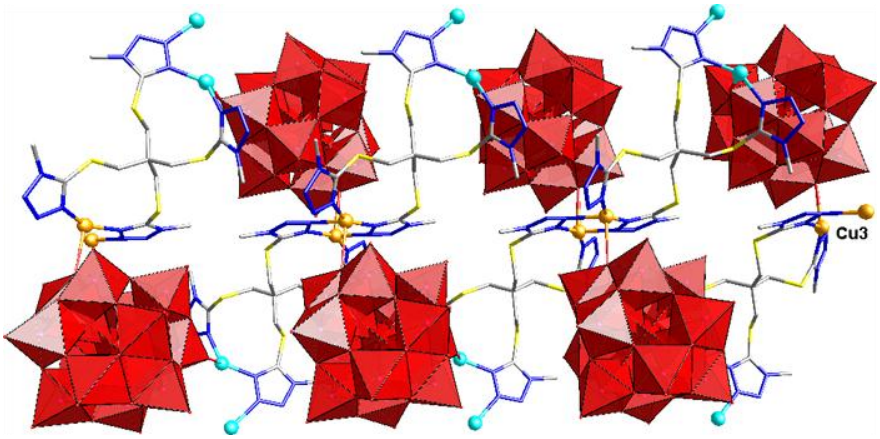

Fig. S21. The neighboring dimer-5 structures link together by sharing two Cu3 ions (orange) to generate a straight chain in compound **3**.

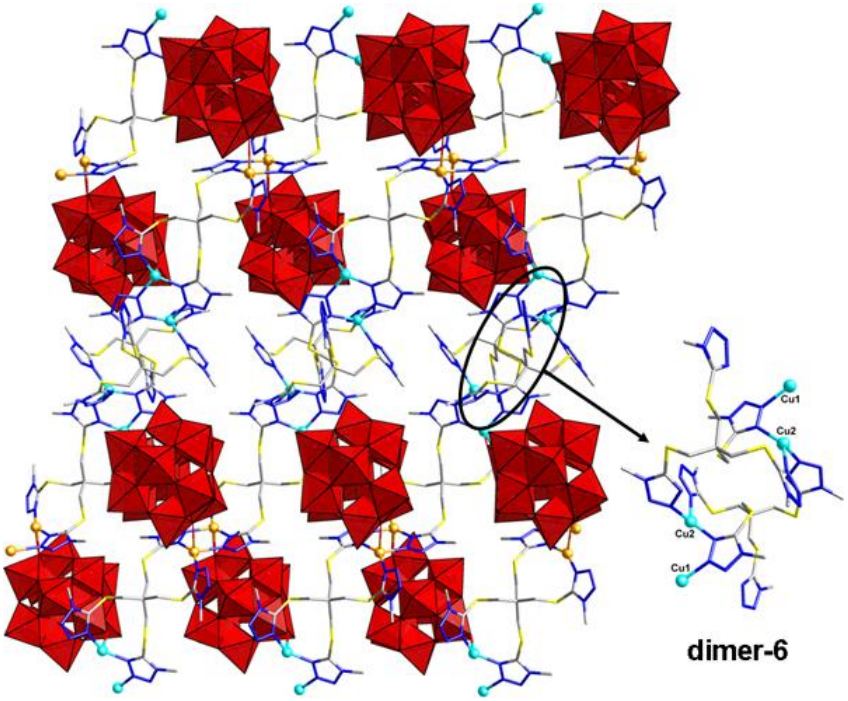

Fig. S22. Diagram illustrating the 2D layer in compound **3** which is constructed by straight chains and dimer-6 units. The dimer-6 unit is constructed by two bpbb[6] ligands.

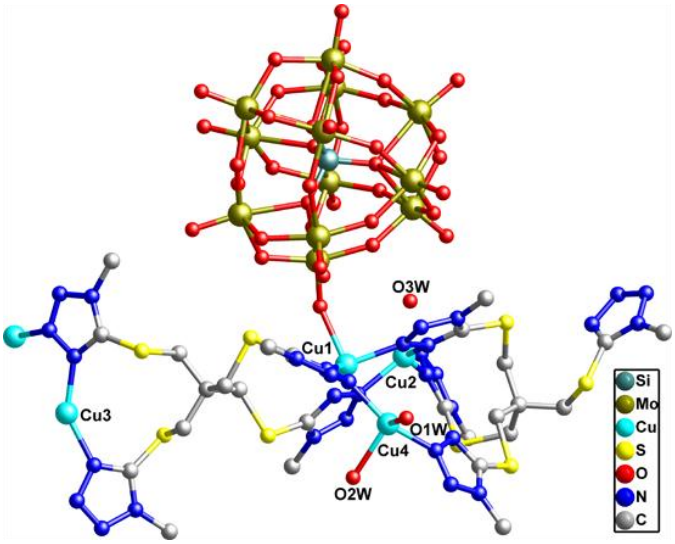

Fig. S23. Ball-and-stick view of the asymmetric unit of compound **4**. All H atoms are omitted for clarity.

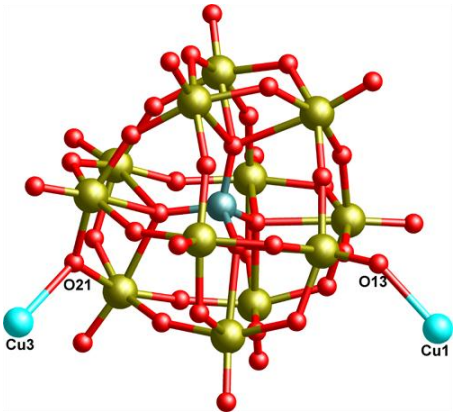

Fig. S24. View of coordination details of Keggin type polyoxoanion $SiMo_{12}$ in compound **4**. Cu1 and Cu3 atoms are coordinated through the terminal O13 and bridging O21 atoms.

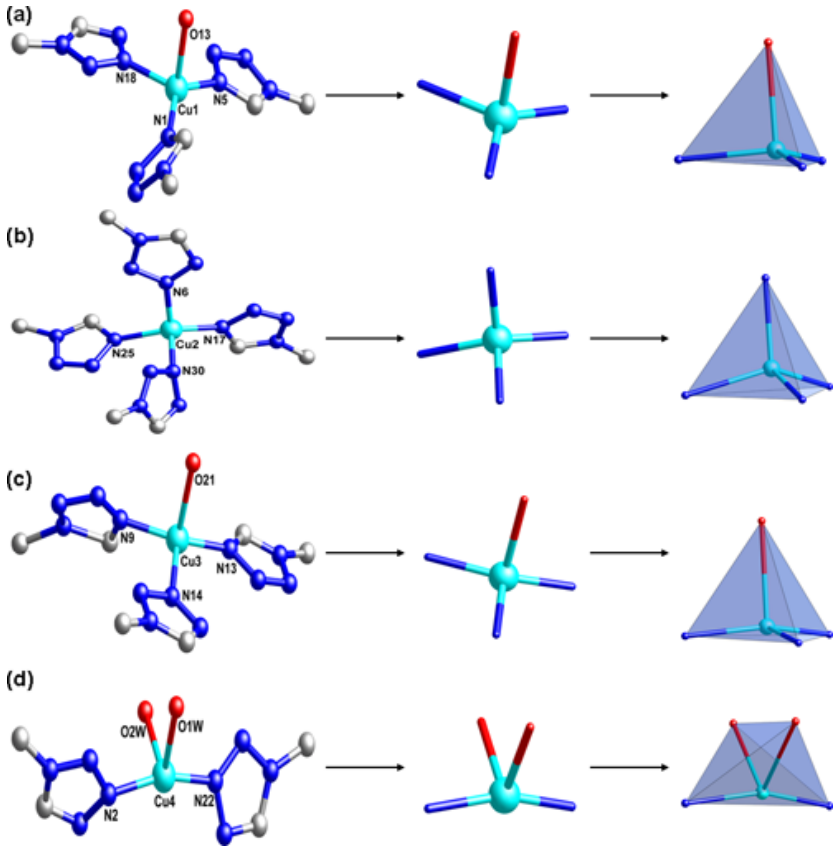

Fig. S25. The coordination details and modes of Cu^{+} ions in compound **4** (a) Cu1 (b) Cu2 (c) Cu3 (d) Cu4.

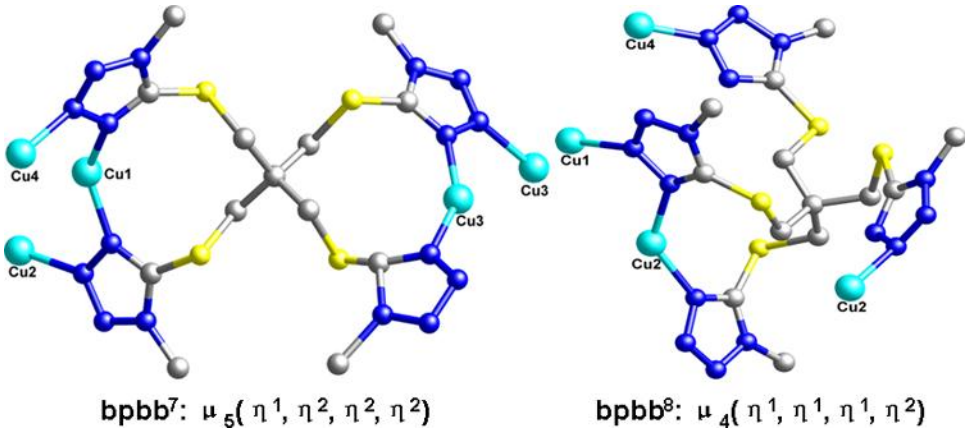

Fig. S26. The coordination modes of multiplex bpbb ligand in compound **4**.

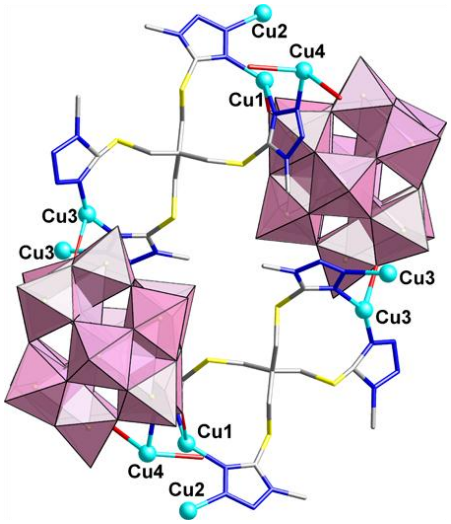

Fig. S27. Ball-and-stick and polyhedral representation of the dimer-7 structure in compound **4**.

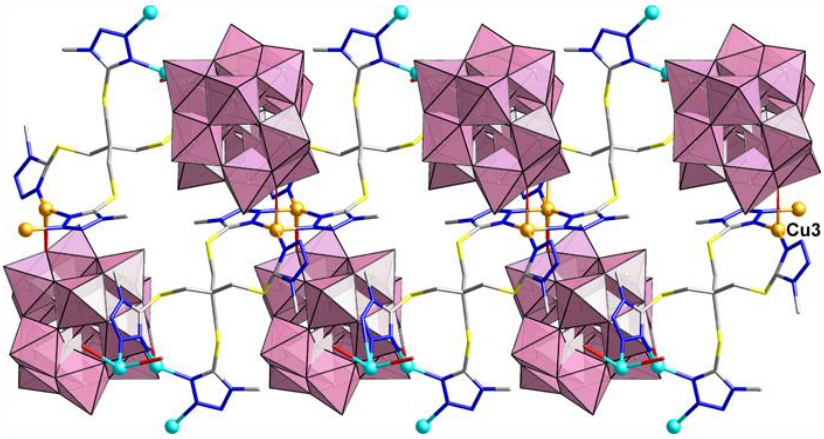

Fig. S28. The neighboring dimer-7 structures link together by sharing two Cu3 ions (orange) to generate a straight chain in compound **4**.

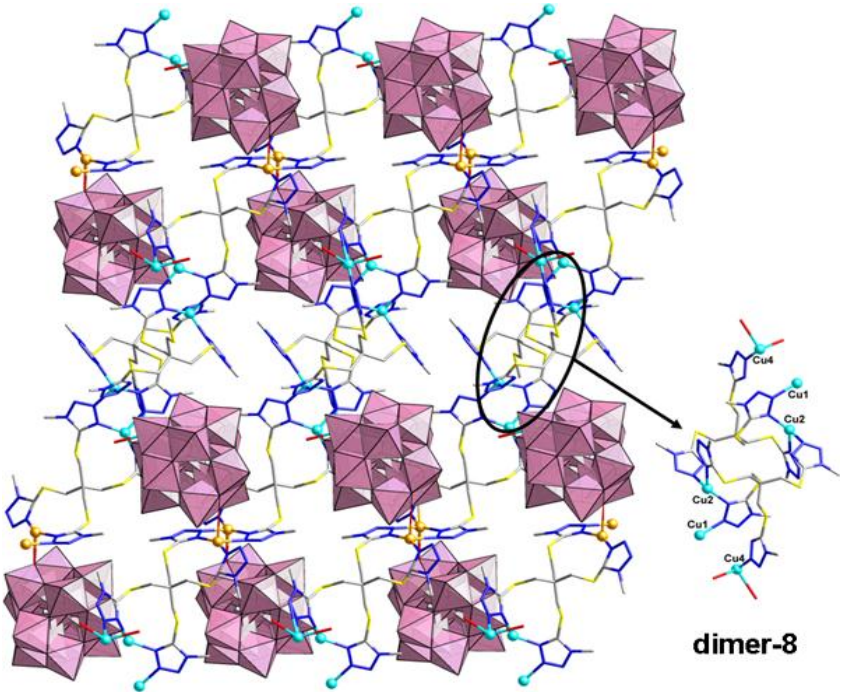

Fig. S29. Diagram illustrating of the 2D layer in compound **4** which is constructed by straight chains and dimer-8 units. The dimer-8 unit is constructed by two bpbb[8] ligands.

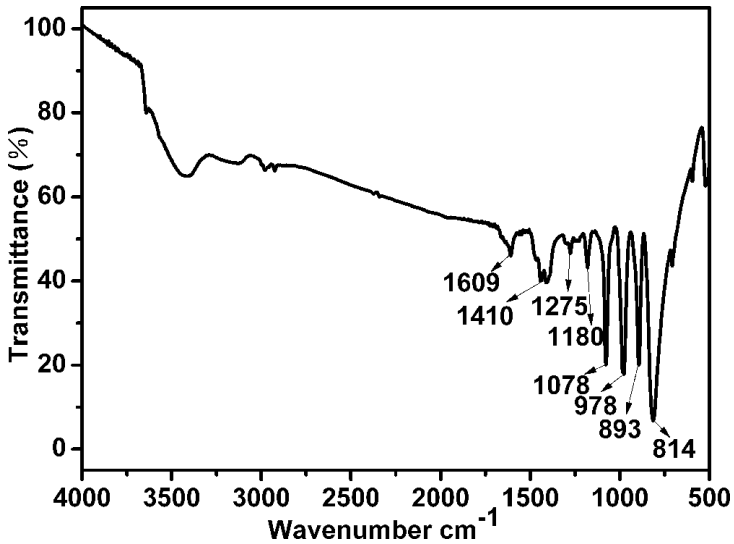

Fig. S30. The IR spectrum of compound **1** exhibits four characteristic asymmetric vibrations resulting from the $[PW_{12}O_{40}]^{3-}$ polyanion. The characteristic bands at 814, 893, 978 and 1078 cm^{-1} are attributed to ν(W-O_t), ν(W-O_b-W), ν(W-O_c-W) and ν(P-O), respectively. The bands in the range of 1180–1609 cm^{-1} are assigned to the vibrations of bpbb ligands.

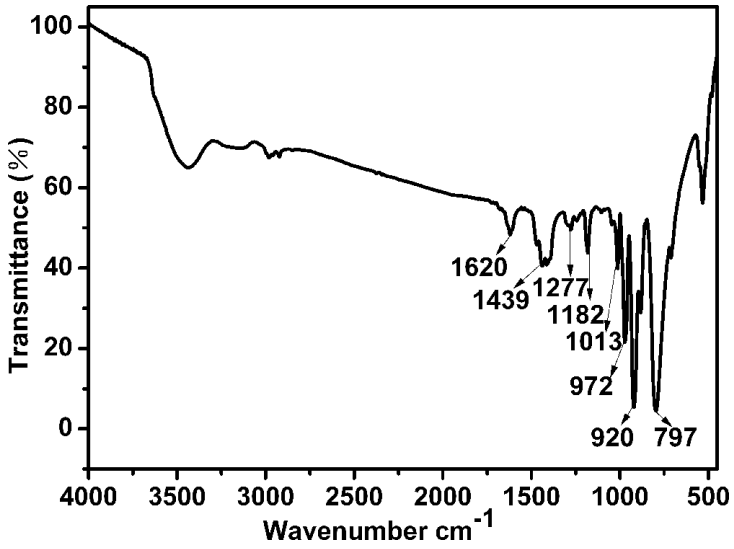

Fig. S31. The IR spectrum of compound **2** exhibits four characteristic asymmetric vibrations resulting from the $[SiW_{12}O_{40}]^{4-}$ polyanion. The characteristic bands at 797, 920, 972 and 1013 cm^{-1} are attributed to ν(W-O_t), ν(W-O_b-W), ν(W-O_c-W) and ν(Si-O), respectively. The bands in the range of 1182–1620 cm^{-1} are assigned to the vibrations of bpbb ligands.

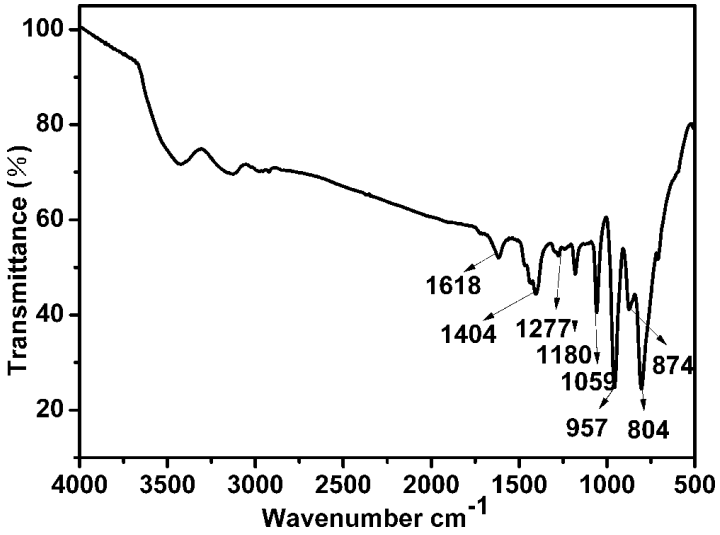

Fig. S32. The IR spectrum of compound **3** exhibits four characteristic asymmetric vibrations resulting from the $[PMo_{12}O_{40}]^{3-}$ polyanion. The characteristic bands at 804, 874, 957 and 1059 cm^{-1} are attributed to ν(Mo-O_t), ν(Mo-O_b-Mo), ν(Mo-O_c-Mo) and ν(P-O), respectively. The bands in the range of 1180–1618 cm^{-1} are assigned to the vibrations of bpbb ligands.

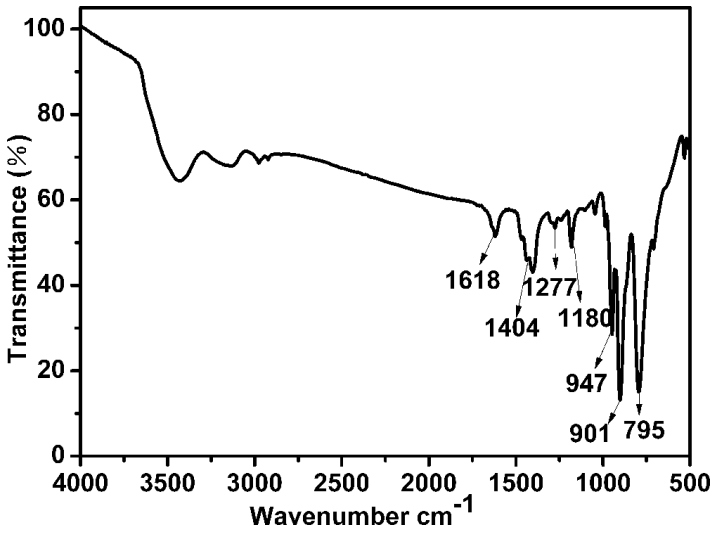

Fig. S33. The IR spectrum of compound **4** exhibits three characteristic asymmetric vibrations resulting from the $[SiMo_{12}O_{40}]^{4-}$ polyanion. The characteristic bands at 795, 901 and 947 cm^{-1} are attributed to ν(Mo-O_t), ν(Mo-O_b-Mo), ν(Mo-O_c-Mo) and ν(Si-O), respectively. The bands in the range of 1180–1618 cm^{-1} are assigned to the vibrations of bpbb ligands.

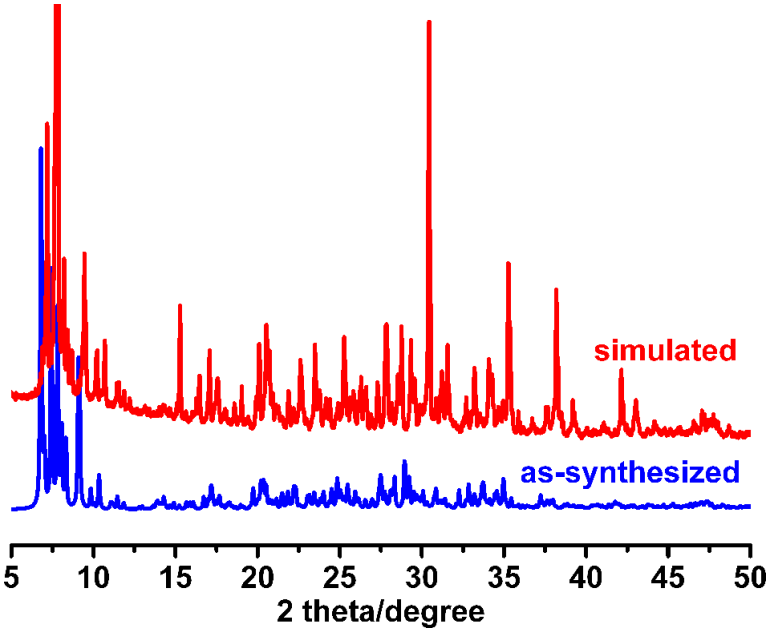

Fig. S34. Experimental XRD patterns of compound **1** exposed in air (blue) and simulation patterns of compound **1** (red).

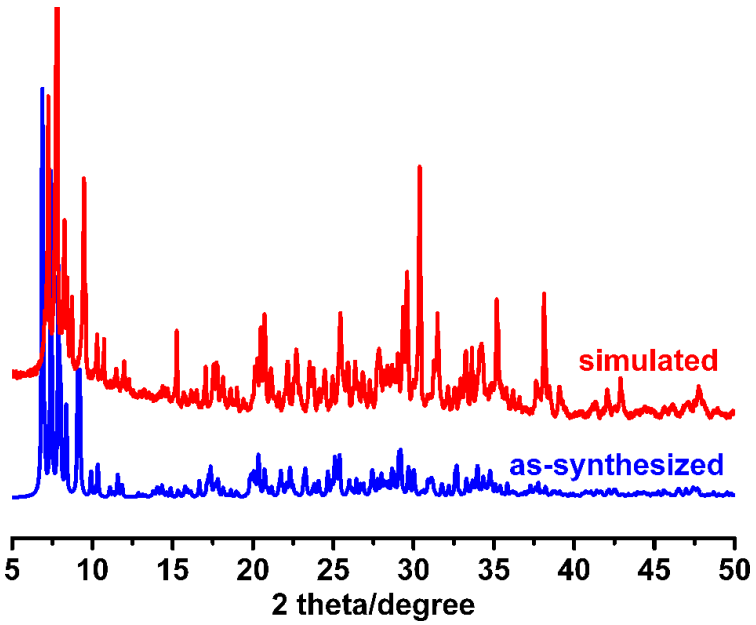

Fig. S35. Experimental XRD patterns of compound **2** exposed in air (blue) and simulation patterns of compound **2** (red).

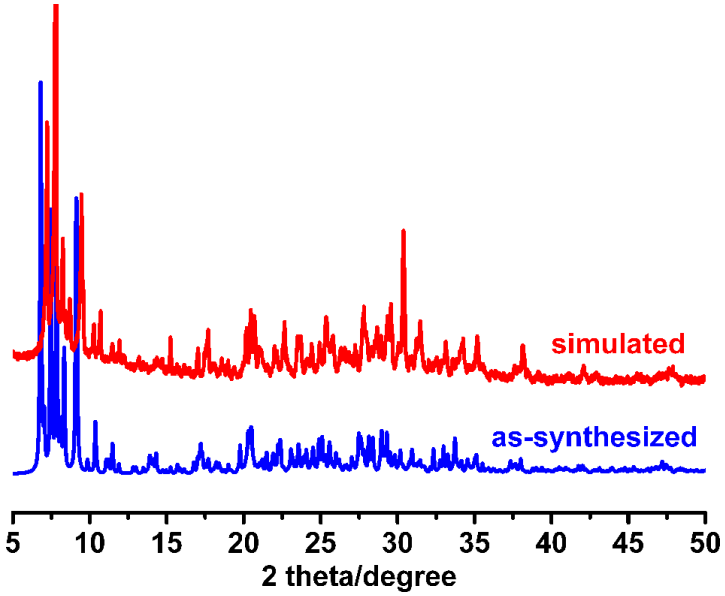

Fig. S36. Experimental XRD patterns of compound **3** exposed in air (blue) and simulation patterns of compound **3** (red).

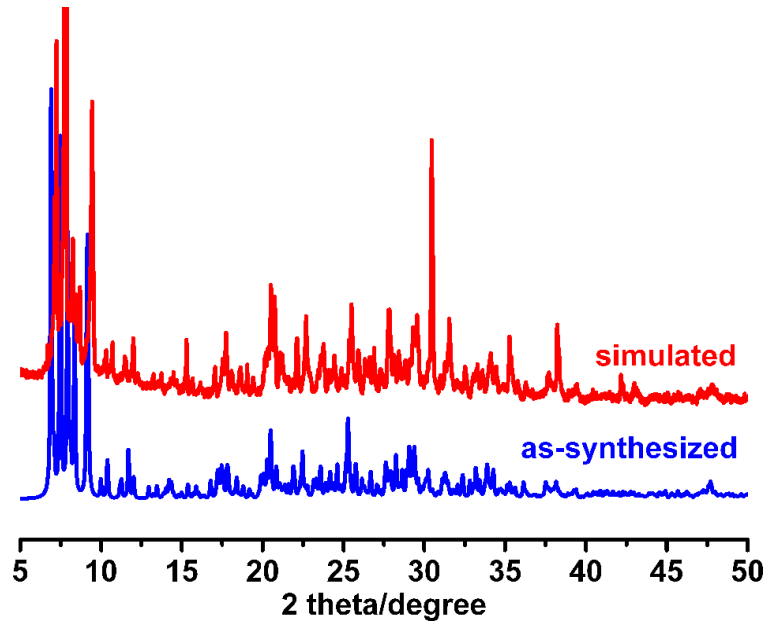

Fig. S37. Experimental XRD patterns of compound **4** exposed in air (blue) and simulation patterns of compound **4** (red).

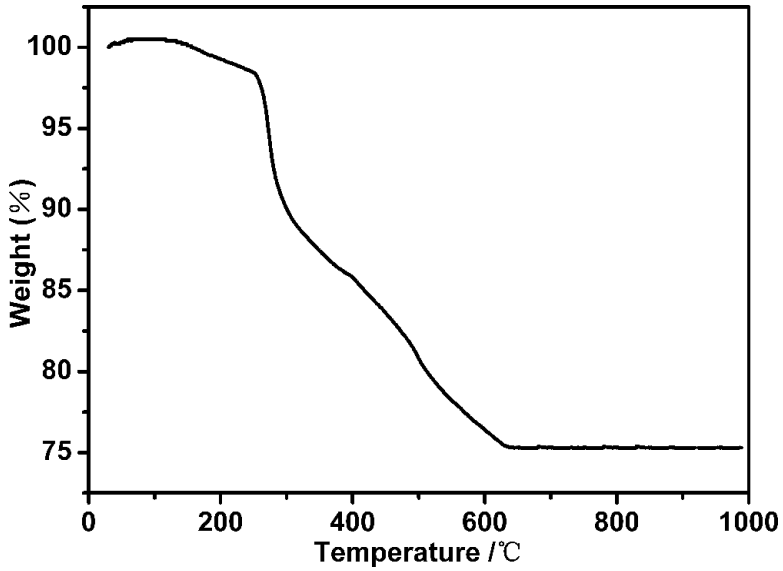

Fig. S38. TG experiments of compound **1** were performed under N_2 atmosphere with a heating rate of 10 ℃/min in the temperature range of 0-1000 ℃. The TG curve indicates that water molecules are eliminated from the network (calcd 1.29%; found 1.56%) when the temperature is increased from room temperature to about 250 °C. The weight loss of 24.16% (calc. 25.27%) from 250 to 630 ℃ corresponds to the loss of bpbb molecules.

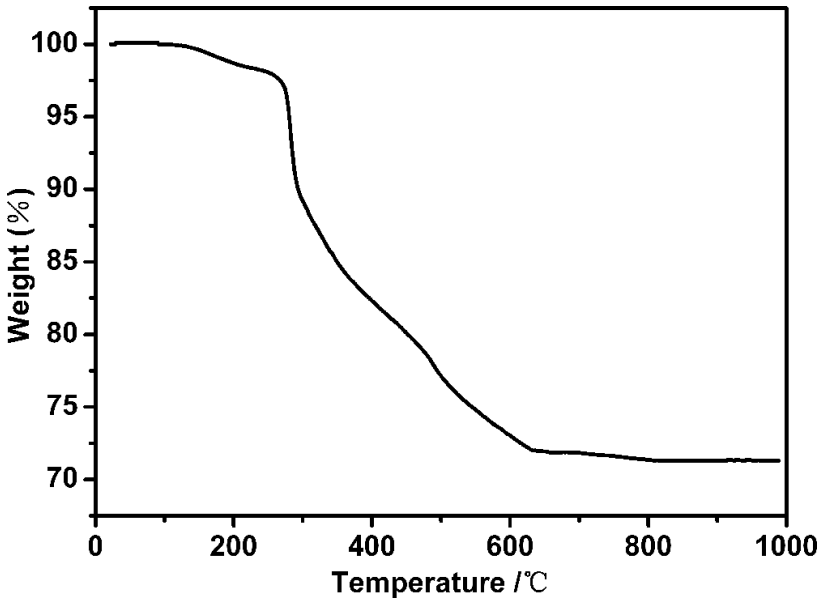

Fig. S39. TG experiments of compound **2** were performed under N_2 atmosphere with a heating rate of 10 ℃/min in the temperature range of 0-1000 ℃. The TG curve indicates that water molecules are eliminated from the network (calcd 1.27%; found 1.95%) when the temperature is increased from room temperature to about 250 °C. The weight loss of 25.85% (calc. 24.91%) from 250 to 630 ℃ corresponds to the loss of bpbb molecules.

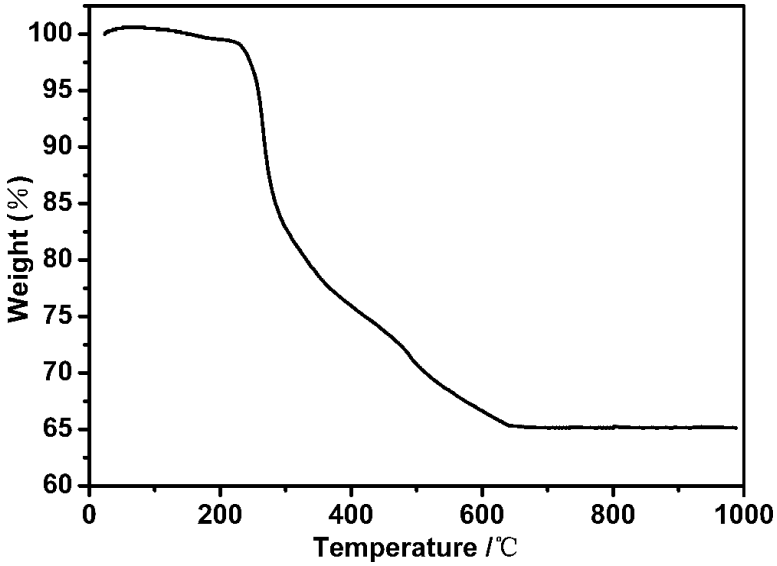

Fig. S40. TG experiments of compound **3** were performed under N_2 atmosphere with a heating rate of 10 ℃/min in the temperature range of 0-1000 ℃. The TG curve indicates that water molecules are eliminated from the network (calcd 1.73%; found 2.98%) when the temperature is increased from room temperature to about 250 °C. The weight loss of 32.24% (calc. 33.80%) from 250 to 630 ℃ corresponds to the loss of bpbb molecules.

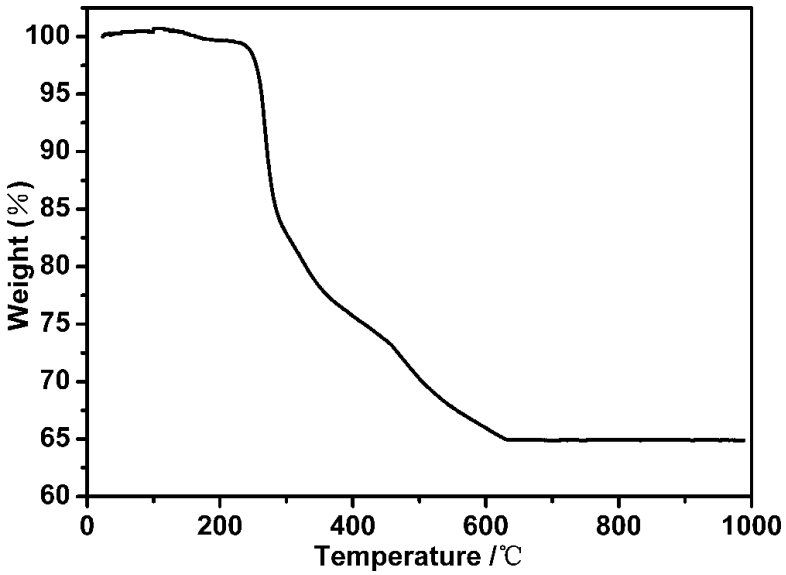

Fig. S41. TG experiments of compound **4** were performed under N_2 atmosphere with a heating rate of 10 ℃/min in the temperature range of 0-1000 ℃. The TG curve indicates that water molecules are eliminated from the network (calcd 1.70%; found 1.83%) when the temperature is increased from room temperature to about 250 °C. The weight loss of 33.42% (calc. 33.16%) from 250 to 630 ℃ corresponds to the loss of bpbb molecules.